Super-Hydrophobic and Resilient Hybrid Silica Aerogels for Thermal Insulation, Energy Harvesting, and Electrical Applications in Harsh Environments

Sasan Rezaei†, Hosseinali Omranpour†, Zeineb Ben Rejeb, Maryam Fashandi, Ali Reza Monfared, Reza Rahmati, Mohammad M. Rastegardoost, Hani E. Naguib, Chul B. Park*

Department of Mechanical and Industrial Engineering, University of Toronto, Toronto, Ontario, Canada, M5S 3G8

*Corresponding Author: park@mie.utoronto.ca

†These two authors contributed equally to this work

Morphological analysis:

The Density Functional Theory (DFT) method stands as a potent tool for determining pore size distributions in nanoporous solid materials. It has demonstrated its efficacy in providing a quantitative description of low-temperature N_2 adsorption on various materials. For accurately assessing pore size and pore size distribution (PSD) in materials featuring nanopores (those with widths smaller than 100 nm), methods grounded in statistical mechanics and molecular simulation, such as DFT, represent the current state-of-the-art. DFT-based techniques are widely embraced and commercially available across numerous gas adsorption systems used for measurement purposes. They offer a reliable means to estimate PSD over a range encompassing micro and mesopores. In contrast, classic methods like Barrett-Joyner-Halenda (BJH), Horvath-Kawazoe (HK), Saito-Foley (SF), and Dubinin-Radushkevich (DR) may not be suitable for the entire nanopore spectrum and have the potential to underestimate pore sizes below 10 nm in width. Considering these factors, and in alignment with the recommendations of the International Standard Organization (ISO), we have chosen to implement DFT as the preferred method for PSD measurements in this paper[1,2].

During gas adsorption, a monolayer is formed on the sorbent's structure in low relative pressure. As the relative pressure is increased, fine pores are filled first, followed by the gas condensation and saturation of all pores. Consequently, the isotherm required for pore structure analysis is obtained. The DFT model considers the properties of the condensed gas on the pores such as the gas density to study the pore properties. The DFT, considers a specific geometry for each material type (i.e., slit for carbon-based, cylinder for silica based, etc.) and fits its theoretical isotherm to the data obtained from the experimental nitrogen adsorption isotherm using complicated fitting and regression procedures. The DFT model can be explained using Equation (1):

$$N_{exp}(P/P_0) = \int_{D_m}^{D_M} N_{DFT}(P/P_0, D) \times F(D) dD \quad (1)$$

where $N_{exp}(P/P_0)$ is the experimental adsorption isotherm, *f(D)* is a pore diameter distribution function, and D_m and D_M are minimum and maximum pore diameters in our model[2]. The basic formulations of the DFT approach can be found elsewhere[3,4].

It is also worth mentioning that there is no distinct relationship between the pore width, pore volume and specific surface area. By assuming all pores having a cylindrical shape, the following equation can be used to estimate the pore size[5]:

$$D_{pore} \approx \frac{V_{pore}}{4S_{BET}} \quad (2)$$

Equation 2 shows that pore width is a function of both pore volume and specific surface area. Hence, improvement of surface area or pore volume will not necessarily affect the pore width.

Thermal imaging experiments:

To conduct thermal imaging experiments, a thick insulation material with tubular hole was affixed to the hot plate to control heat convection. Subsequently, the samples were placed within this hole, and temperature at the center of each sample was recorded. In thermal images, the red circle is the visible portion of the hot plate. This circle served as a visual indicator for the reference temperature.

Figure S1. The optical images of the samples depict the diverse degrees of contraction.

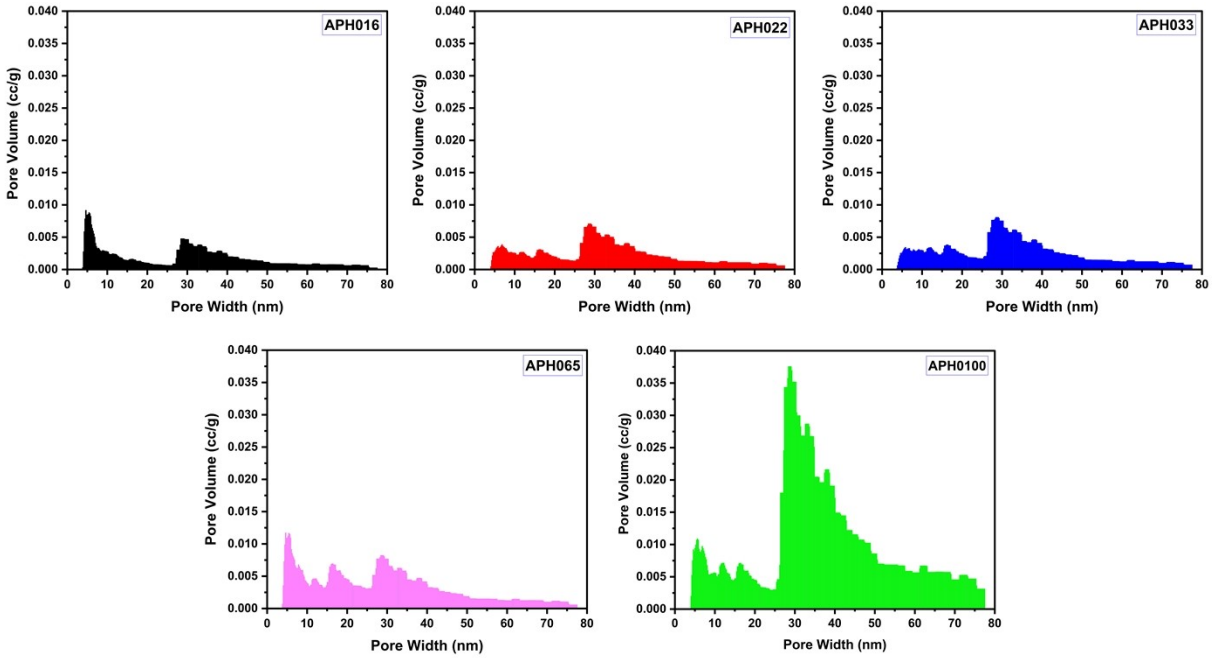

Figure S2: Linear pore size distribution and related pore volume for all samples.

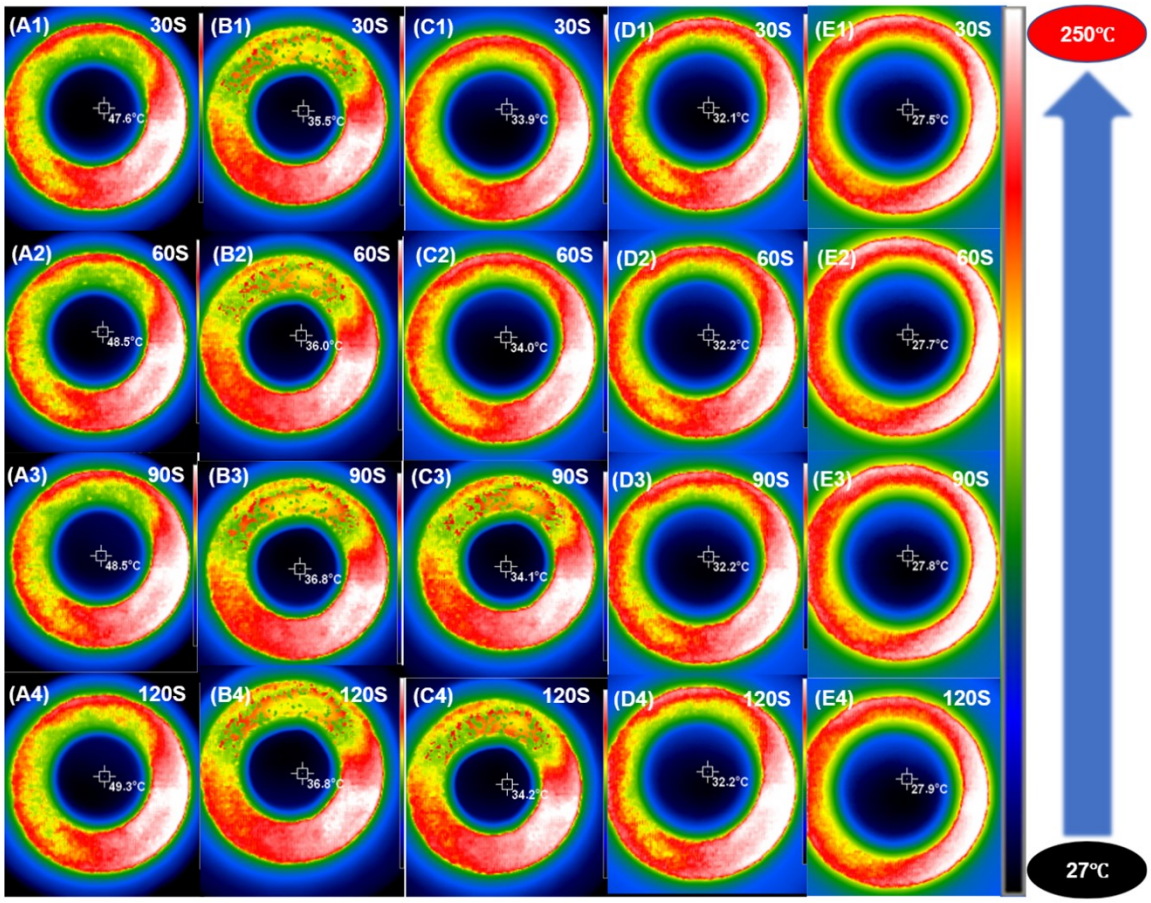

Figure S3. Thermal images of the samples captured at 30-second intervals, APH016 (A1-A4), APH022 (B1-B4), APH033 (C1-C4), APH065 (D1-D4), APH100 (E1-E4)

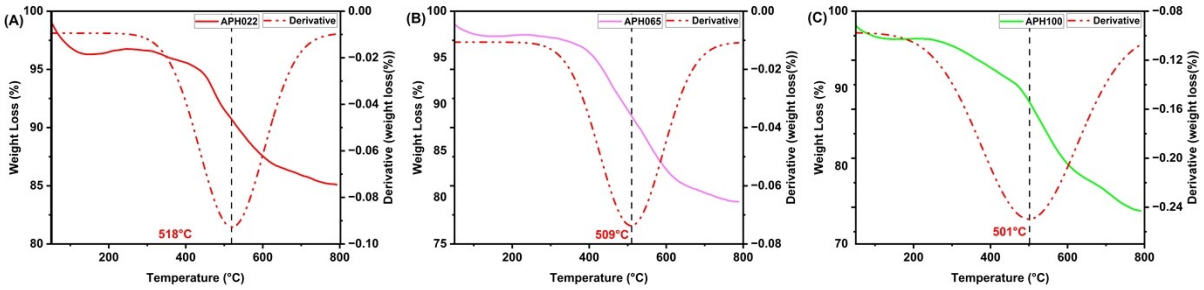

Figure S4. Thermal stability analyzed using TGA curves and their derivatives.

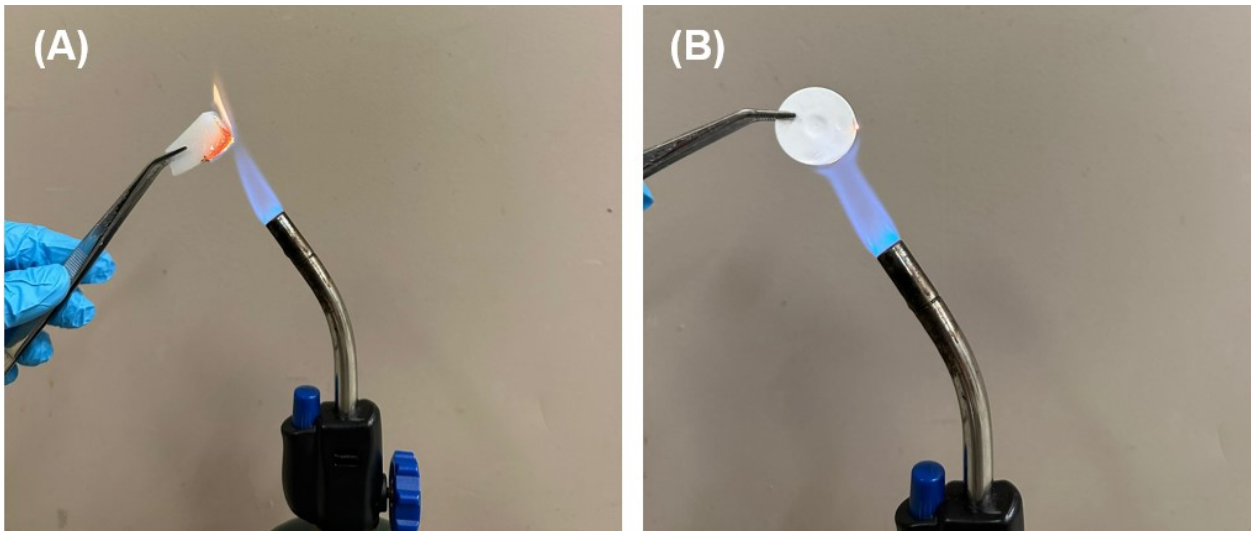

Figure S5. (A) PVTMS sample burns in fire, while (B) APH016 is more fire resistant.

Densification Modulus:

The densification modulus was computed for all specimens following the curvature point of the diagrams. In order to maintain consistency in the measurement procedure, reference points of 1 and 3.3 MPa were selected, except for sample APH022HC, where the maximum point is at 2.12 MPa.

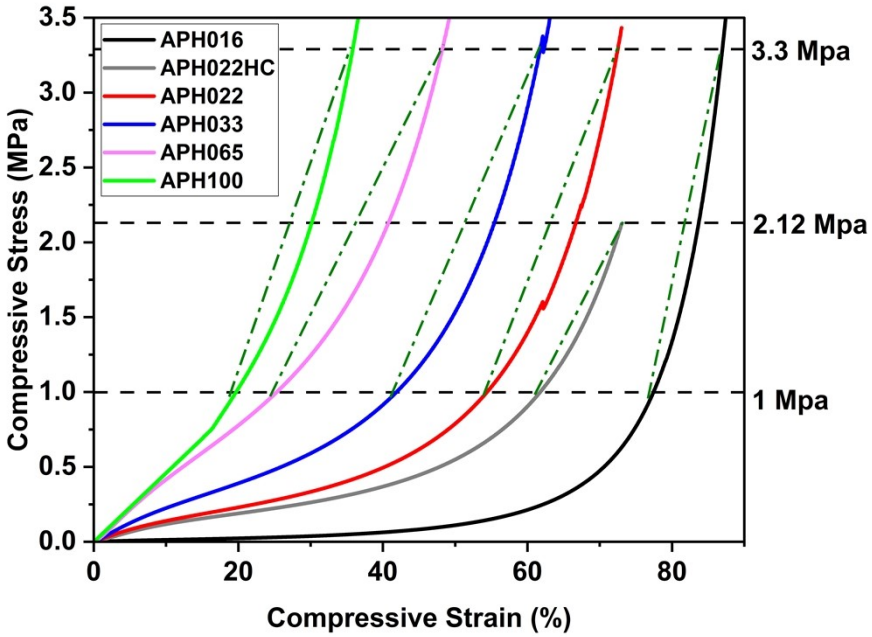

Figure S6. Densification modulus for specimens.

Table S1: Stress-strain values for calculating young and densification modulus and data points for comparing samples at 15, 25, and 35 % strain.

APH016		APH022HC		APH022		APH033		APH065		APH100	
Strain (%)	**Stress (Mpa)**	**Strain (%)**	**Stress (Mpa)**	**Strain (%)**	**Stress (Mpa)**	**Strain (%)**	**Stress (Mpa)**	**Strain (%)**	**Stress (Mpa)**	**Strain (%)**	**Stress (Mpa)**
0	0	0	0	0	0	0	0	0	0	0	0
0.99	0.00	1.00	0.01	0.99	0.02	0.99	0.02	0.99	0.03	0.99	0.04
1.00	0.00	1.02	0.01	1.01	0.02	1.01	0.02	1.01	0.03	1.01	0.05
15.00	0.02	15.01	0.16	15.01	0.19	15.01	0.31	15.01	0.59	15.01	0.69
25.00	0.03	25.01	0.22	25.00	0.28	25.00	0.48	25.00	0.99	25.01	1.47
35.00	0.05	35.01	0.31	35.01	0.40	35.01	0.73	35.01	1.58	35.00	3.09
77.45	1.00	61.77	1.00	54.40	1.00	41.90	1.00	25.32	1.00	19.69	1.00
86.99	3.30	73.04	2.12	72.55	3.30	61.79	3.30	48.30	3.30	35.87	3.30

References:

1 ISO 15901-2:2022 - Pore size distribution and porosity of solid materials by mercury porosimetry and gas adsorption — Part 2: Analysis of nanopores by gas adsorption, https://www.iso.org/standard/67586.html.

2 R. Bardestani, G. S. Patience and S. Kaliaguine, *Can J Chem Eng*, 2019, **97**, 2781–2791.

3 J. Landers, G. Y. Gor and A. V. Neimark, *Colloids Surf A Physicochem Eng Asp*, 2013, **437**, 3–32.

4 P. I. Ravikovitch, G. L. Haller and A. V. Neimark, *Adv Colloid Interface Sci*, 1998, **76–77**, 203–226.

5 H. Maleki, S. Montes, N. Hayati-Roodbari, F. Putz and N. Huesing, *ACS Appl Mater Interfaces*, 2018, **10**, 22718–22730.